Japanese Journal of Applied Physics **58**, 068004 (2019) **BRIEF NOTE**
https://doi.org/**10.7567/1347-4065/ab0784**

First demonstration of Brillouin optical correlation-domain reflectometry based on external modulation scheme

Kohei Noda*, Heeyoung Lee, Yosuke Mizuno, and Kentaro Nakamura

Institute of Innovative Research, Tokyo Institute of Technology, Yokohama 226-8503, Japan

*E-mail: knoda@sonic.pi.titech.ac.jp

Received December 19, 2018; revised February 8, 2019; accepted February 15, 2019; published online May 28, 2019

We demonstrate basic operation of Brillouin optical correlation-domain reflectometry (BOCDR) based on an external modulation scheme, which can mitigate three demerits of a conventional direct modulation scheme. A 0.8 m long strain in a 2.8 m long silica fiber is successfully detected in a distributed manner. This scheme can be employed not only in BOCDR but also in Brillouin optical correlation-domain analysis.
© 2019 The Japan Society of Applied Physics

Supplementary material for this article is available online

Fiber-optic distributed strain and temperature sensing techniques based on Brillouin scattering have been extensively studied, and a number of configurations have been developed, including time-, frequency-, and correlation-domain techniques.[1–14] Here, we focus on Brillouin optical correlation-domain reflectometry (BOCDR), which has general merits such as operation by single-end light injection, high spatial resolution, random accessibility, and cost efficiency.[15,16] Since the first proposal of BOCDR, its performance has been drastically improved; for instance, ultrahigh-speed distributed sensing was demonstrated in 2016.[17]

All of the previously reported configurations of BOCDR have been based on a direct modulation scheme, in which the driving current of a laser is directly modulated to generate frequency-modulated light.[15–17] However, despite its cost efficiency, the direct modulation scheme poses three problems: (1) a suitable laser for high-speed large-amplitude modulation needs to be selected, (2) optical power modulation is inevitably accompanied, possibly resulting in deteriorated performance, and (3) the modulation amplitude is strongly dependent on the modulation frequency, possibly leading to a significant change in spatial resolution according to measurement position.

These drawbacks are also found in optical correlation-domain reflectometry (OCDR),[18–23] which is a Fresnel-reflection-based technique for detecting low-quality connections, splices, and damaged parts along an optical fiber. We have developed a new OCDR configuration based on an external modulation scheme, in which, instead of directly modulating the driving current of a laser, the optical frequency is modulated using an electro-optic modulator (EOM).[24] After demonstrating basic operation of external-modulation-based OCDR, we have proved that at least two drawbacks (1) and (3) can be mitigated.[24]

However, in the external modulation scheme, the power of the frequency-modulated light becomes significantly low because of the limited modulation efficiency of an EOM and the insertion loss of an optical narrowband-pass filter. Therefore, although the external-modulation-based operation of OCDR with relatively strong reflected signal has been already verified, that of BOCDR with relatively weak signal has not been demonstrated yet.

In this study, by appropriately amplifying the frequency-modulated light, we demonstrate basic operation of BOCDR based on the external modulation scheme for the first time to the best of our knowledge. We show that, when strain of up to 0.71% is applied to a 0.8 m long section of a 2.8 m long sensing fiber, the obtained distributions of the Brillouin gain spectrum (BGS) and the Brillouin frequency shift (BFS) are in good agreement with the simulation results.

BOCDR is a single-end-access distributed strain and temperature sensing technique based on synthesis of an optical coherence function (SOCF).[25] By sinusoidally modulating the optical frequency of a laser output, a so-called correlation peak is generated along a sensing fiber. By controlling the modulation frequency, the position of the correlation peak can be scanned along the fiber, enabling distributed measurement. The spatial resolution and measurement range are determined by the modulation frequency and amplitude; refer to the previous literatures[15,16] for more details. Conventionally, the frequency-modulated light was generated by directly modulating the driving current of a laser. This direct modulation scheme is cost-efficient but suffers from the aforementioned demerits. Here, we employ the external modulation scheme, in which the optical frequency of the laser output is constant, while it is sinusoidally modulated using an external EOM.

The experimental setup of external-modulation-based BOCDR, depicted in Fig. 1(a), is basically identical to that previously reported[15,16] except for the preparation of the frequency-modulated light (before its division into pump and reference lights). To modulate the frequency of the laser output (NX8563LB, NEC), first, a frequency-swept sawtooth electrical signal was generated using a function generator (FG) and applied to a voltage-controlled oscillator (VCO; HMC733LC4B, Analog Devices). Then the frequency-modulated microwave output from the VCO was applied to a double-sideband modulator (DSBM), and the generated upper sideband was selected using an optical narrowband-pass filter (BVF-300CL, Alnair). The generated frequency-modulated light, which was significantly weak (<-20 dBm), was boosted to 8 dBm using an erbium-doped fiber amplifier (EDFA) and an optical filter for suppressing amplified spontaneous emission. The polarization state was scrambled. The power of the incident light to the sensing fiber was 27 dBm. Spectral averaging was performed four times. The modulation frequency was swept from 4.15 MHz to 4.21 MHz, and the modulation amplitude was approximately 1.4 GHz, corresponding to the spatial resolution of approximately 0.24 m and the measurement range of 24 m

 © 2019 The Japan Society of Applied Physics

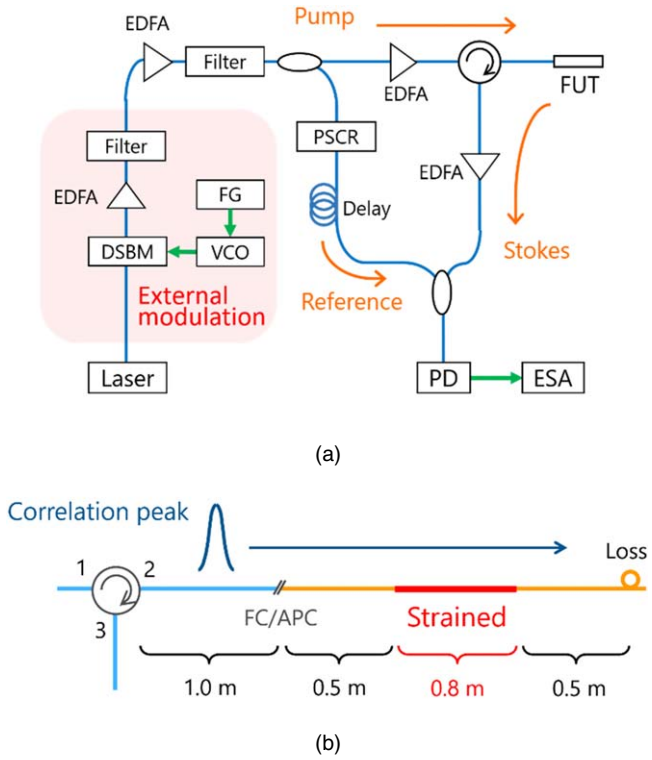

Fig. 1. (Color online) Schematic setup. (a) Setup of BOCDR based on external modulation scheme. DSBM: double-sideband modulator, EDFA: erbium-doped fiber amplifier, ESA: electrical spectrum analyzer, FG: function generator, FUT: fiber under test. PD: photo diode, PSCR: polarization scrambler, VCO: voltage-controlled oscillator. (b) Structure of sensing fiber.

(calculated using equations in Refs. 15 and 16; note that the dependence of the spatial resolution on the measurement position is much smaller than that of the direct modulation scheme).[24)]

The structure of the sensing fiber is depicted in Fig. 1(b). A 1.8 m long unjacketed silica single-mode fiber (SMF; BFS = 10.84 GHz, pre-measured strain dependence coefficient of BFS = 448 MHz/%) was connected to a 1.0 m long jacketed silica SMF of the second port of an optical circulator (BFS = 10.87 GHz) via a ferrule connector/angled physical contact (FC/APC) connector and employed as a sensing fiber. A considerable bending loss was artificially applied near the end of the fiber to suppress the Fresnel reflection. Part of the sensing fiber was fixed on a translational stage using a clump, and strains of up to 0.71% were applied to a 0.8 m long section of the fiber. We applied strain to a fiber section much longer than the spatial resolution to demonstrate distributed sensing with a high signal-to-noise ratio. The room temperature was 22 °C.

The measured BGS and BFS distributions when 0.46% strain was applied are shown in Fig. 2. The vertical axis was normalized so that the maximal and minimal powers of each BGS became 1 and 0, respectively. The relative position was defined as the distance from the circulator. In the strained section, the BFS changed for approximately 200 MHz. The slight change of the BFS at the position = 1.0 m corresponds to the aforementioned slight difference of the BFSs of the two different silica SMFs.

Subsequently, we measured the BFS distributions when strain was varied from 0 to 0.71% [Fig. 3(a)]. As strain increased, the BFS in the strained section also increased. The BFS (calculated as an average of the BFS values in the 30-cm-long section at the middle of the strained section) was plotted as a function of applied strain, as shown in Fig. 3(b). The dependence was almost linear, and the coefficient was 419 MHz/%, which moderately agrees with the theoretical value pre-measured using the whole length. Thus, the basic operation, i.e., distributed strain measurement, was experimentally demonstrated by external-modulation-based BOCDR. Note that comparative study on the direct modulation scheme and the external modulation scheme is also provided in the online supplementary data available online at stacks.iop.org/JJAP/58/068004/mmedia.

In conclusion, the basic operation of BOCDR based on the external modulation scheme was demonstrated for the first time. A 0.8 m long strain in a 2.8 m long sensing fiber was successfully detected. This scheme can mitigate the general

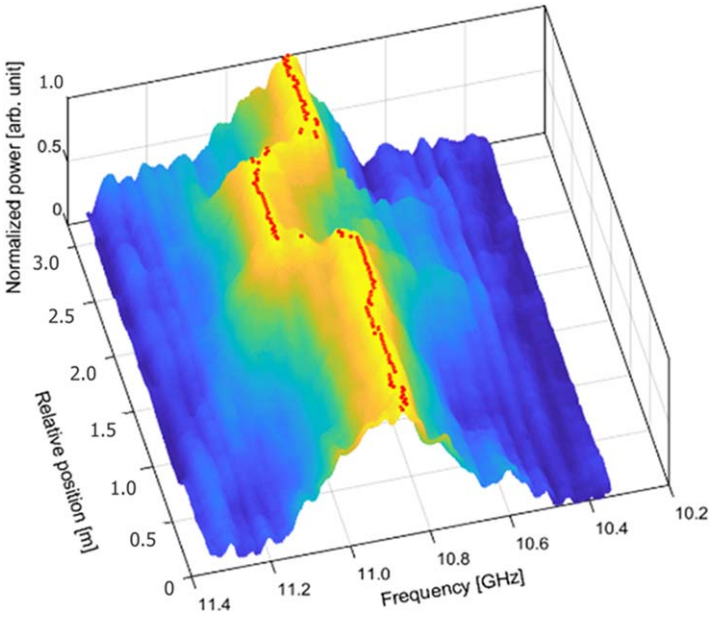

Fig. 2. (Color online) Normalized BGS distribution measured at 0.46% strain. The BFS distribution is also indicated in red.

© 2019 The Japan Society of Applied Physics

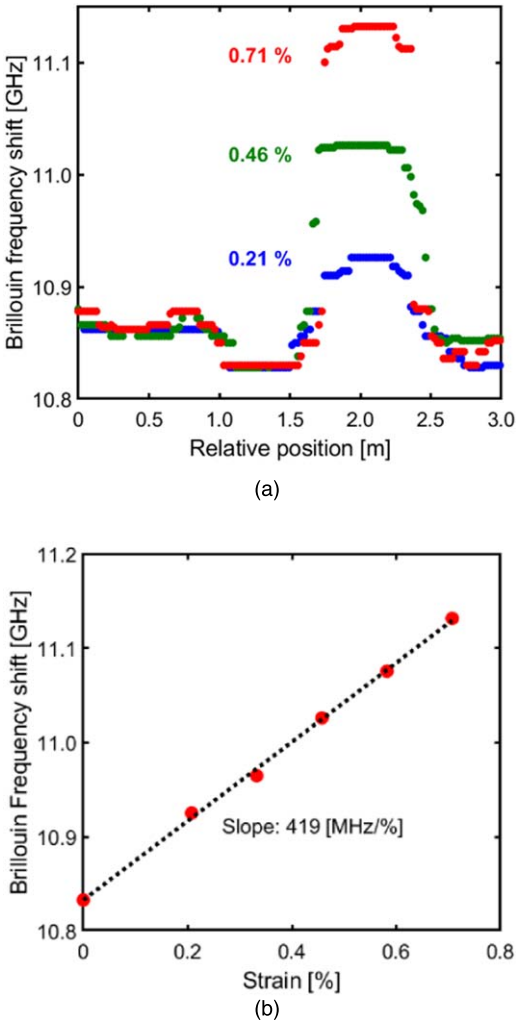

Fig. 3. (Color online) Experimental results. (a) BFS distributions when strain was changed from 0 to 0.71%. (b) BFS (in the strained section) plotted as a function of applied strain.

demerits of the conventional direct modulation scheme. Specifically speaking, a laser which is not designed for high-frequency large-amplitude modulation can be used. In addition, this scheme is free from the nonlinear mutual dependence between the modulation frequency and amplitude, and unexpected change in the spatial resolution according to the measurement position can be avoided. The influence of the power modulation, which is inevitably accompanied in the direct modulation scheme, will also be mitigated, though further study is required on this point. We note that this external modulation scheme is applicable not only to BOCDR but also to Brillouin optical correlation-domain analysis (BOCDA).[11–14] Thus, we anticipate that the first demonstration of the external-modulation-based distributed Brillouin measurement is an important technological step in optical fiber sensing community.

Acknowledgments This work was supported by JSPS KAKENHI Grant No. 17H04930 and 17J07226 and by a research grant from the Fujikura Foundation.

ORCID iDs Kohei Noda https://orcid.org/0000-0003-4976-9657 Heeyoung Lee https://orcid.org/0000-0003-3179-0386 Yosuke Mizuno https://orcid.org/0000-0002-3362-4720 Kentaro Nakamura https://orcid.org/0000-0003-2899-4484

1) G. P. Agrawal, *Nonlinear Fiber Optics* (Academic, San Diego, CA, 1995).
2) A. H. Hartog, *An Introduction to Distributed Optical Fibre Sensors* (CRC Press, Boca Raton, FL, 2017).
3) M. Nikles and F. Ravet, Nat. Photon. **4**, 431 (2010).
4) T. Horiguchi and M. Tateda, J. Lightwave Technol. **7**, 1170 (1989).
5) R. Bernini, A. Minardo, and L. Zeni, Opt. Lett. **34**, 2613 (2009).
6) Y. Peled, A. Motil, and M. Tur, Opt. Express **20**, 8584 (2012).
7) M. Taki, Y. Muanenda, C. J. Oton, T. Nannipieri, A. Signorini, and F. Di Pasquale, Opt. Lett. **38**, 2877 (2013).
8) A. Denisov, M. A. Soto, and L. Thevenaz, Light: Sci. Appl. **5**, e16074 (2016).
9) D. Zhou, Y. Dong, B. Wang, C. Pang, D. Ba, H. Zhang, Z. Lu, H. Li, and X. Bao, Light: Sci. Appl. **7**, 32 (2018).
10) D. Garus, K. Krebber, F. Schliep, and T. Gogolla, Opt. Lett. **21**, 1402 (1996).
11) K. Hotate and T. Hasegawa, IEICE Trans. Electron. **E83-C**, 405 (2000).
12) K. Y. Song, Z. He, and K. Hotate, Opt. Lett. **31**, 2526 (2006).
13) Y. H. Kim, K. Lee, and K. Y. Song, Opt. Express **23**, 33241 (2015).
14) W. Zou, C. Jin, and J. Chen, Appl. Phys. Express **5**, 082503 (2012).
15) Y. Mizuno, W. Zou, Z. He, and K. Hotate, Opt. Express **16**, 12148 (2008).
16) Y. Mizuno, W. Zou, Z. He, and K. Hotate, J. Lightwave Technol. **28**, 3300 (2010).
17) Y. Mizuno, N. Hayashi, H. Fukuda, K. Y. Song, and K. Nakamura, Light: Sci. Appl. **5**, e16184 (2016).
18) R. C. Youngquist, S. Carr, and D. E. N. Davies, Opt. Lett. **12**, 158 (1987).
19) T. Okamoto, D. Iida, K. Toge, and T. Manabe, J. Lightwave Technol. **34**, 4259 (2016).
20) M. Shizuka, S. Shimada, N. Hayashi, and K. Nakamura, Appl. Phys. Express **9**, 032702 (2016).
21) M. Shizuka, H. Lee, N. Hayashi, Y. Mizuno, and K. Nakamura, Jpn. J. Appl. Phys. **55**, 128003 (2016).
22) M. Shizuka, N. Hayashi, Y. Mizuno, and K. Nakamura, Appl. Opt. **55**, 3925 (2016).
23) N. Hayashi, M. Shizuka, K. Minakawa, Y. Mizuno, and K. Nakamura, IEICE Electron. Express **12**, 20150824 (2015).
24) K. Noda, G. Han, H. Lee, Y. Mizuno, and K. Nakamura, Appl. Phys. Express **12**, 022005 (2019).
25) K. Hotate, Meas. Sci. Technol. **13**, 1746 (2002).

© 2019 The Japan Society of Applied Physics